

# Обзор ArXiv: astro-ph, 21-25 декабря 2015 года

От Сильченко О.К.

# Astro-ph: 1512.06268

## Evolution of Galaxy Shapes from Prolate to Oblate through Compaction Events

Matteo Tomassetti<sup>1,2\*</sup>, Avishai Dekel<sup>1†</sup>, Nir Mandelker<sup>1</sup>, Daniel Ceverino<sup>3</sup>, Sharon Lapiner<sup>1</sup>, Sandra Faber<sup>2</sup>, Omer Kneller<sup>1</sup>, Joel Primack<sup>2</sup>, Tanmayi Sai<sup>2</sup>

<sup>1</sup> *Center for Astrophysics and Planetary Science, Racah Institute of Physics, The Hebrew University, Jerusalem 91904, Israel*

<sup>2</sup> *Department of Physics, University of California, Santa Cruz, CA 95064, USA*

<sup>3</sup> *Universität Heidelberg, Zentrum für Astronomie, Institut für Theoretische Astrophysik, Albert-Ueberle-Str. 2, 69120 Heidelberg,*

# Эволюция через «голубой орешек»

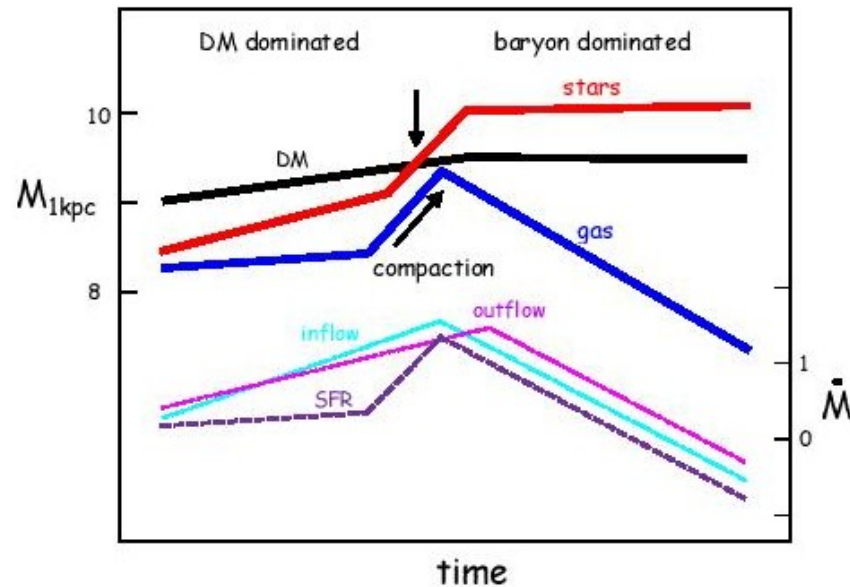
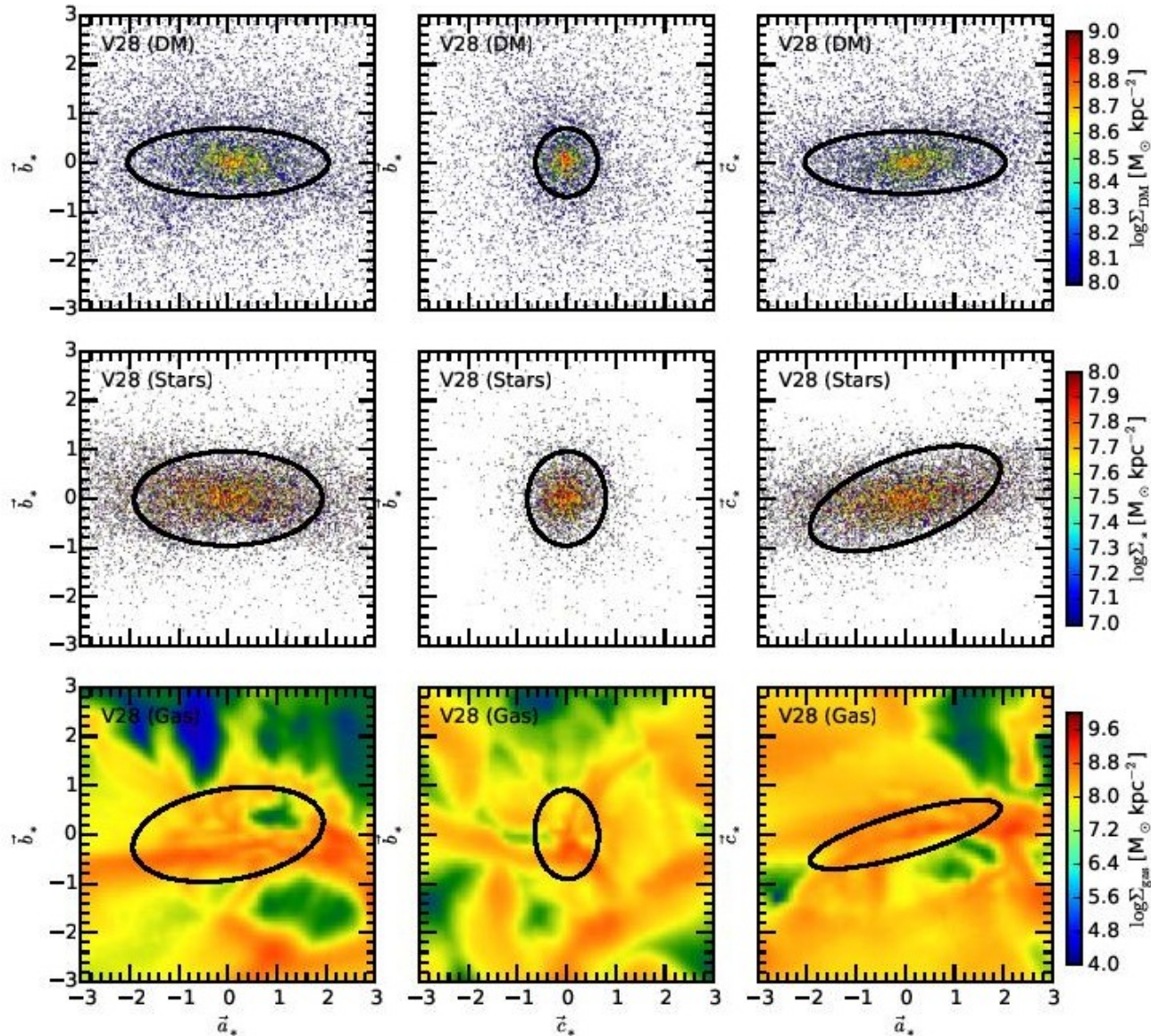


**Figure 1.** Characteristic evolution of masses and their rates of change within the central regions of the galaxies in our simulations (according to the analysis of [Zolotov et al. \(2015\)](#) and [Tacchella et al. \(2015b\)](#)). After an early phase of gradual mass growth and star formation, there is a well-defined, relatively short phase of wet compaction in the inner 1 kpc, reaching a peak of central gas density and SFR (a blue nugget). After that, there is a longer phase of gas depletion and quenching of SFR caused by a low rate of inflow to the center compared to the sum of SFR and outflow rate. The result is a compact quenched galaxy (a red nugget), where the central stellar density remains roughly constant from the blue nugget phase and one.

# Форма: звезды повторяют темную материю, газ – холодные потоки



### 3.2 The Shape Parameters

The shape of an ellipsoid with axes  $a \geq b \geq c$  can be characterized by two axial ratios, e.g.

$$q = \frac{b}{a}, \quad p = \frac{c}{b}, \quad (4)$$

each ranging from 0 to 1.

An ellipsoid is oblate if  $q < p$  and it is prolate if  $p < q$ . Extreme examples are a disk where  $p \ll q \sim 1$  and a filament where  $q \ll p \sim 1$ . When  $p \sim q$  the system is triaxial; it is close to a sphere when  $p \sim q \sim 1$  and it is elongated when  $p \sim q \ll 1$ . For the purpose of a more uniform coverage of the parameter plane, we replace  $q$  and  $p$  by the parameters of *elongation* and *flattening*,

$$e = (1 - q^2)^{1/2}, \quad f = (1 - p^2)^{1/2}, \quad (5)$$

also ranging from 1 to 0, in the opposite sense.

In the plane of  $e$  and  $f$  (as in  $q$  and  $p$ ) the different shapes occupy distinct loci. With  $e$  along the x-axis and  $f$  along the y-axis, oblate systems are at the top-left, prolate systems are at the bottom-right, and triaxial systems are along the diagonal, ranging from spheres at the bottom-left to elongated triaxial at the top-right.

Another common choice is to replace  $p = c/b$  by  $s = c/a$ , and use the *triaxiality* parameter (Franx et al. 1991)

$$T = \frac{1 - q^2}{1 - s^2}, \quad (6)$$

also ranging from 0 to 1. It is common to consider a

# Эволюция формы – от prolate к сфере?

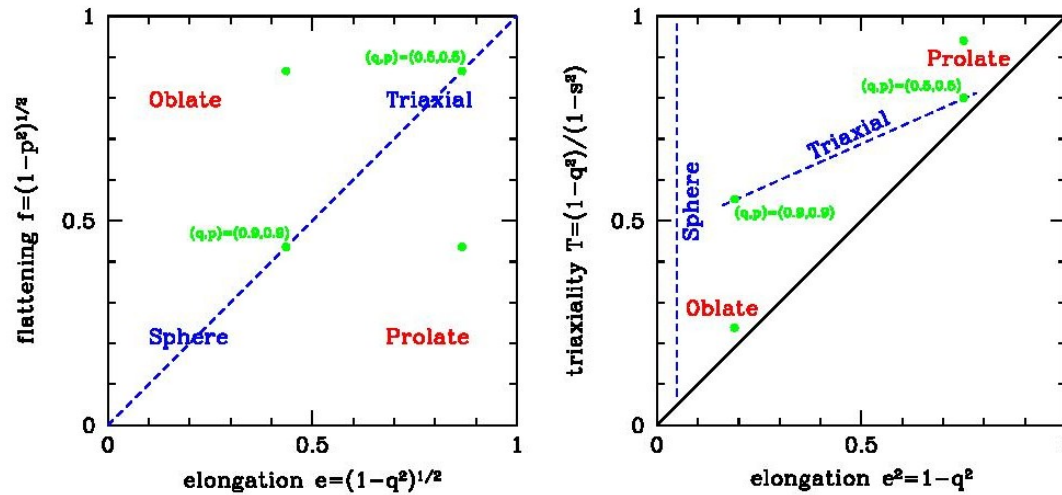


**Figure 2.** Presenting the shape. The left panel shows the elongation versus flattening plane. The blue dashed line is the locus of pure triaxial systems, ranging from a sphere (at the bottom-left corner) to a very elongated triaxial system (at the top-right corner). The line separates oblate and prolate ellipsoids, which lie in the top left and bottom right of the plane, respectively. The green points mark the location on the plane for four different combinations of  $q$  and  $p$  as indicated in parenthesis. The right panel shows the triaxiality versus elongation squared plane. The bottom-right half of the plane is forbidden. A sphere can obtain any value of  $T$ . Triaxial systems lie on a

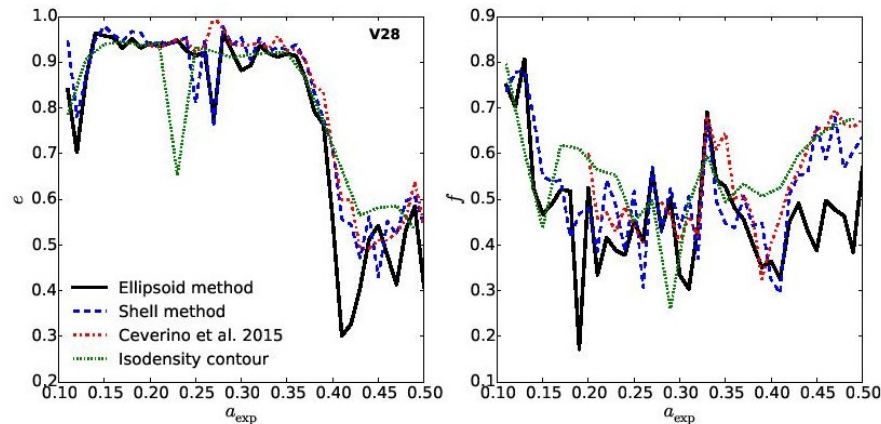
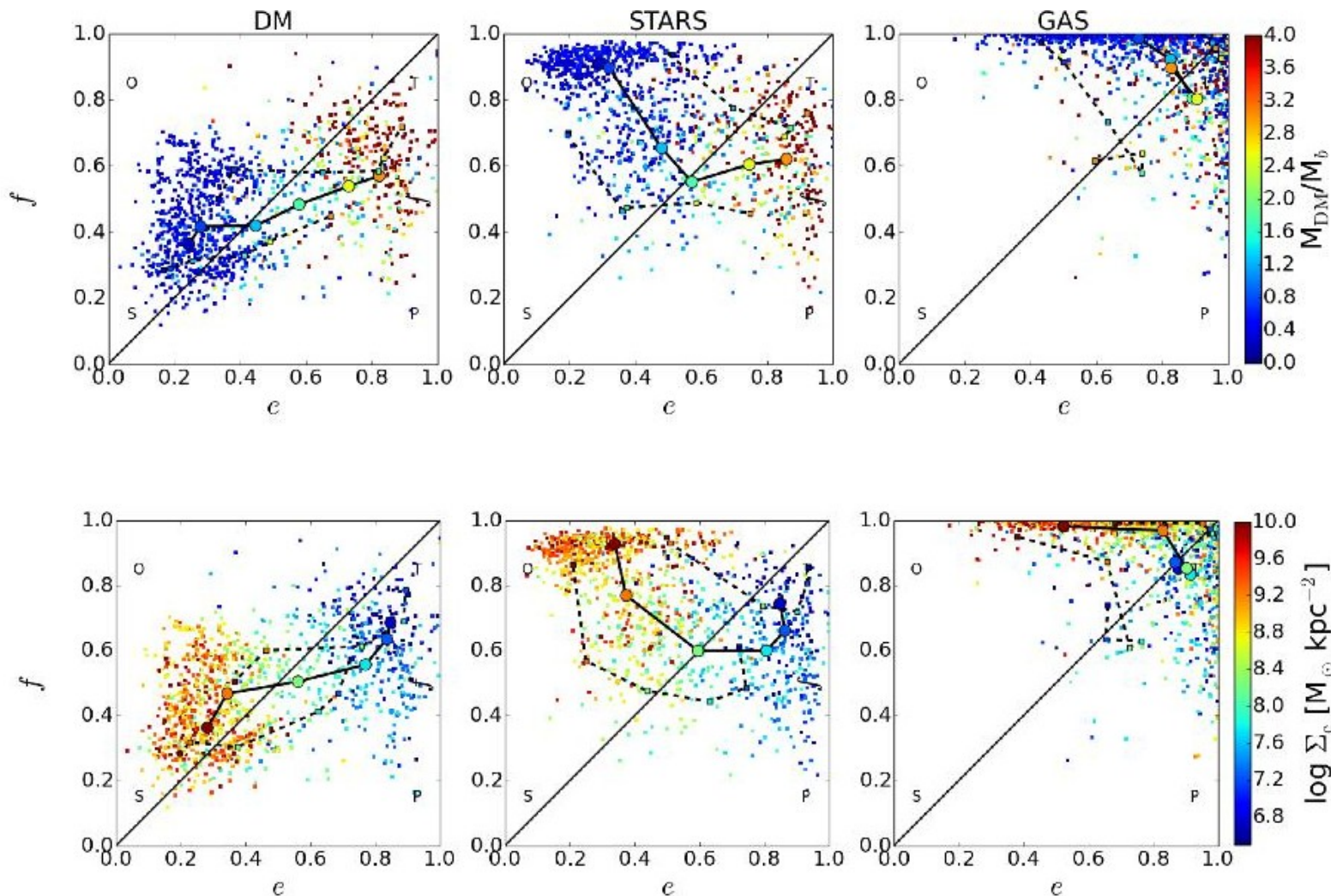


**Figure 3.** Elongation (left panel) and flattening (right panel) as function of the expansion factor for the stellar component of V28. Our

# Эволюция темной материи, звезд и газа



# Astro-ph: 1512.07058

## The flaring HI disk of the nearby spiral galaxy NGC 2683\*

B. Vollmer, F. Nehlig, R. Ibata

Observatoire astronomique de Strasbourg, UMR 7750, 11, rue de l'université, 67000 Strasbourg, France

Received / Accepted

**Abstract.** New deep VLA D array HI observations of the highly inclined nearby spiral galaxy NGC 2683 are presented. Archival C array data were processed and added to the new observations. To investigate the 3D structure of the atomic gas disk, we made different 3D models for which we produced model HI data cubes. The main ingredients of our best-fit model are (i) a thin disk inclined by  $80^\circ$ ; (ii) a crude approximation of a spiral and/or bar structure by an elliptical surface density distribution of the gas disk; (iii) a slight warp in inclination between  $10 \text{ kpc} \leq R \leq 20 \text{ kpc}$  (decreasing by  $10^\circ$ ); (iv) an exponential flare that rises from 0.5 kpc at  $R = 9 \text{ kpc}$  to 4 kpc at  $R = 15 \text{ kpc}$ , stays constant until  $R = 22 \text{ kpc}$ , and decreases its height for  $R > 22 \text{ kpc}$ ; and (v) a low surface-density gas ring with a vertical offset of 1.3 kpc. The slope of NGC 2683's flare is comparable, but



# NGC 2683: spiral edge-on

**Table 1.** Basic parameters of NGC 2683

Type	Sb	
$m_B^0$	9.84 mag	(de Vaucouleurs et al. 1976)
$D_{25}$	$9.3' = 20.8$ kpc	(Nilson 1973)
Distance	7.7 Mpc	(Tonry et al. 2001)
$M_B$	$-19.59$ mag	
$v_{\text{rot}}^{\text{max}}$	$215 \text{ km s}^{-1}$	(Casertano & van Gorkom 1991)
$\dot{M}_*$	$0.8 M_{\odot} \text{ yr}^{-1}$	(Irwin et al. 1999)
$l_B$	$0.81' = 1.8$ kpc	(Kent 1985)
$l_{K'}$	$0.67' = 1.5$ kpc	(this paper)
$M_*$	$3.6 \times 10^{10} M_{\odot}$	(this paper)
$M_{*,\text{disk}}$	$2.6 \times 10^{10} M_{\odot}$	(this paper)

# HI observations:

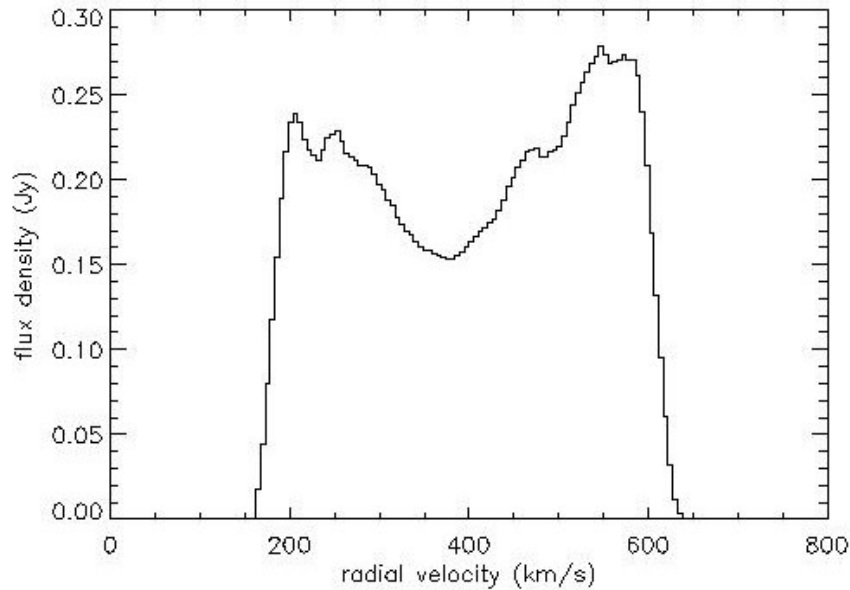


**Fig. 1.** Integrated HI spectrum of NGC 2683 from the VLA D array observations.

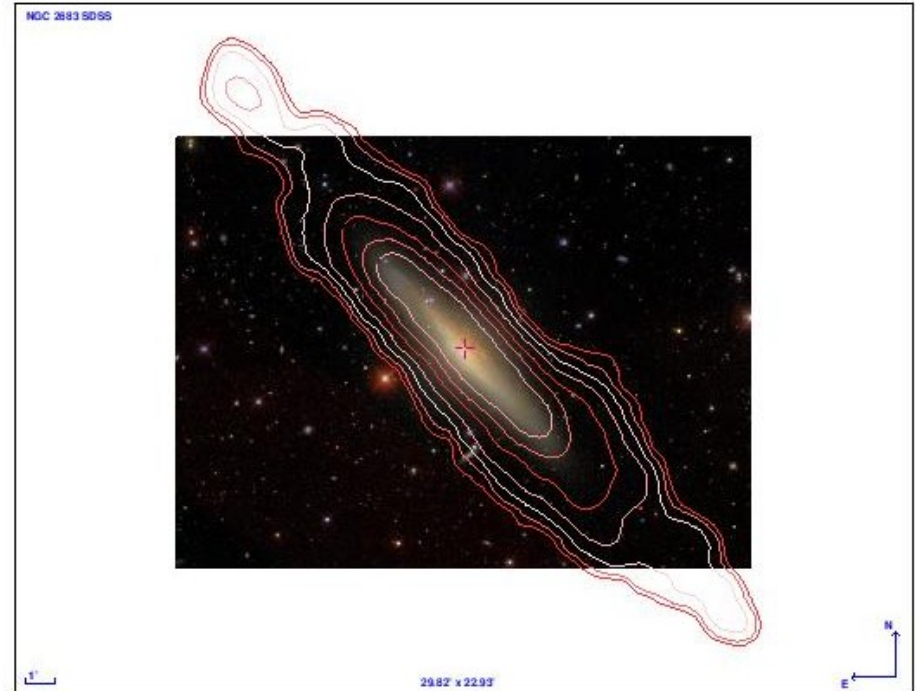
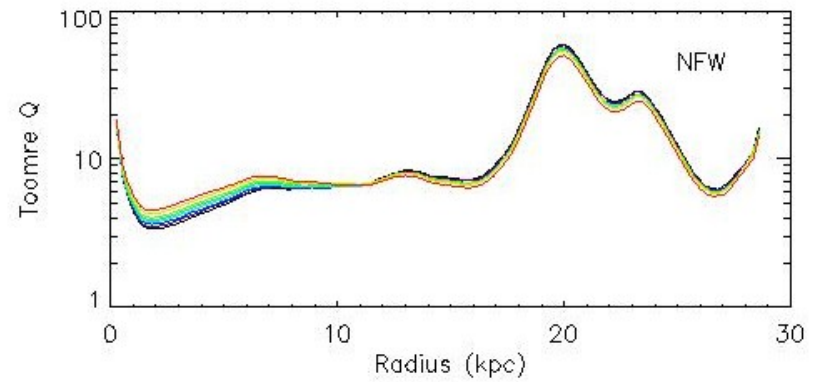
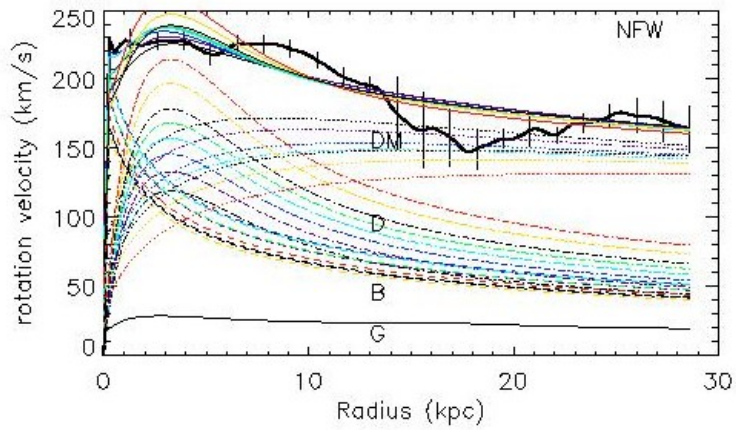
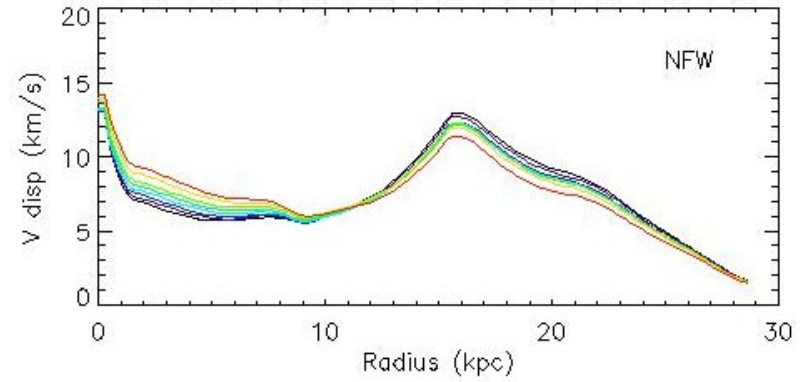
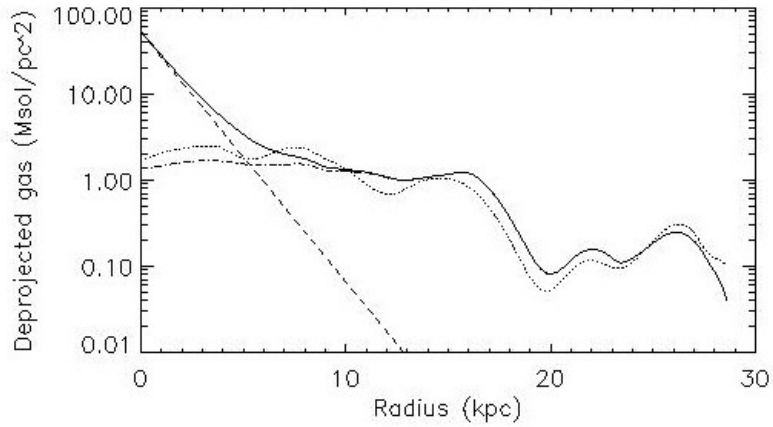


**Fig. 3.** HI contours on the SDSS color image of NGC 2683 (copyright 2006 Michael R. Blanton & David W. Hogg). The contour levels are  $(2,4,8,16,32,64,128) \times$

# Динамика



# Flaring!!

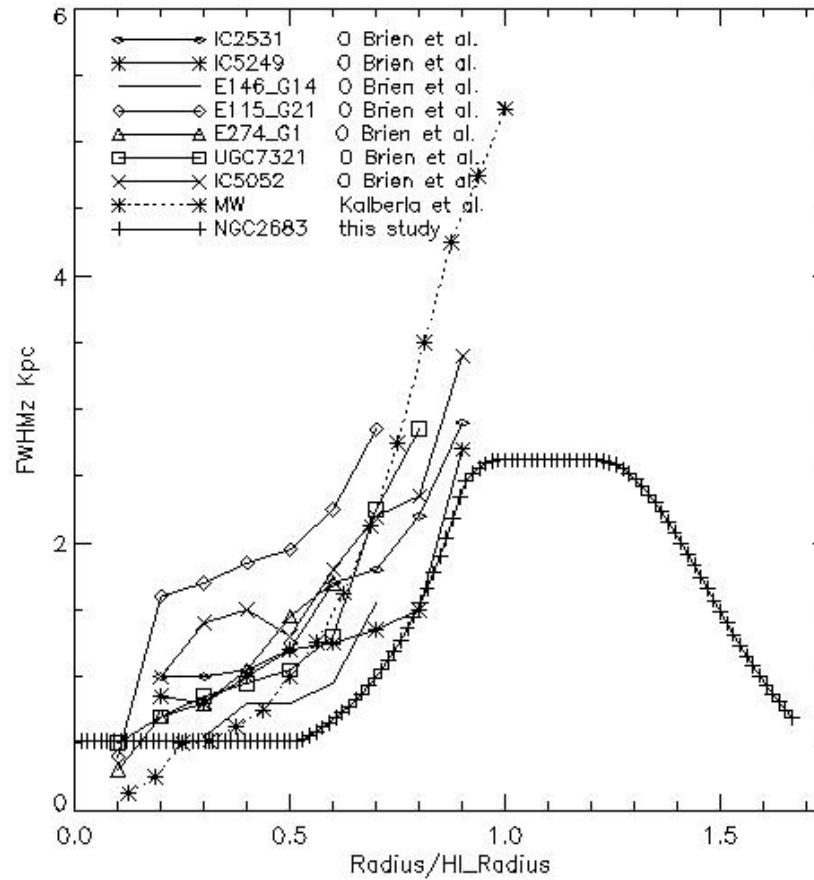


**Fig. 18.** Comparison between the flare of the gas disk and those of other spiral galaxies.

# Astro-ph: 1512.07667

MUSE-INGS ON AM1354-250: COLLISIONS, SHOCKS AND RINGS

BLAIR C. CONN<sup>1</sup>, L.M.R. FOGARTY<sup>2</sup>, RORY SMITH<sup>3,4,5</sup> AND GRAEME N. CANDLISH<sup>5</sup>

*Draft version December 25, 2015*

## ABSTRACT

We present MUSE observations of AM1354-250, confirming its status as a collisional ring galaxy which has recently undergone an interaction, creating its distinctive shape. We analyse the stellar and gaseous emission throughout the galaxy finding direct evidence that the gaseous ring is expanding with a velocity of  $\sim 70 \text{ km.s}^{-1}$  and that star formation is occurring primarily in HII regions associated with the ring. This star formation activity is likely triggered by the interaction. We find evidence for several excitation mechanisms in the gas, including emission consistent with shocked gas in the expanding ring and a region of LINER-like emission in the central core of the galaxy. Evidence of kinematic disturbance in both the stars and gas, possibly also triggered by the interaction, can be seen in all of the velocity maps. The ring galaxy retains weak spiral structure, strongly suggesting the progenitor galaxy was a massive spiral prior to the collision with its companion an estimated  $140 \pm 12$  Myr ago.

# AM 1354-250: collisional ring

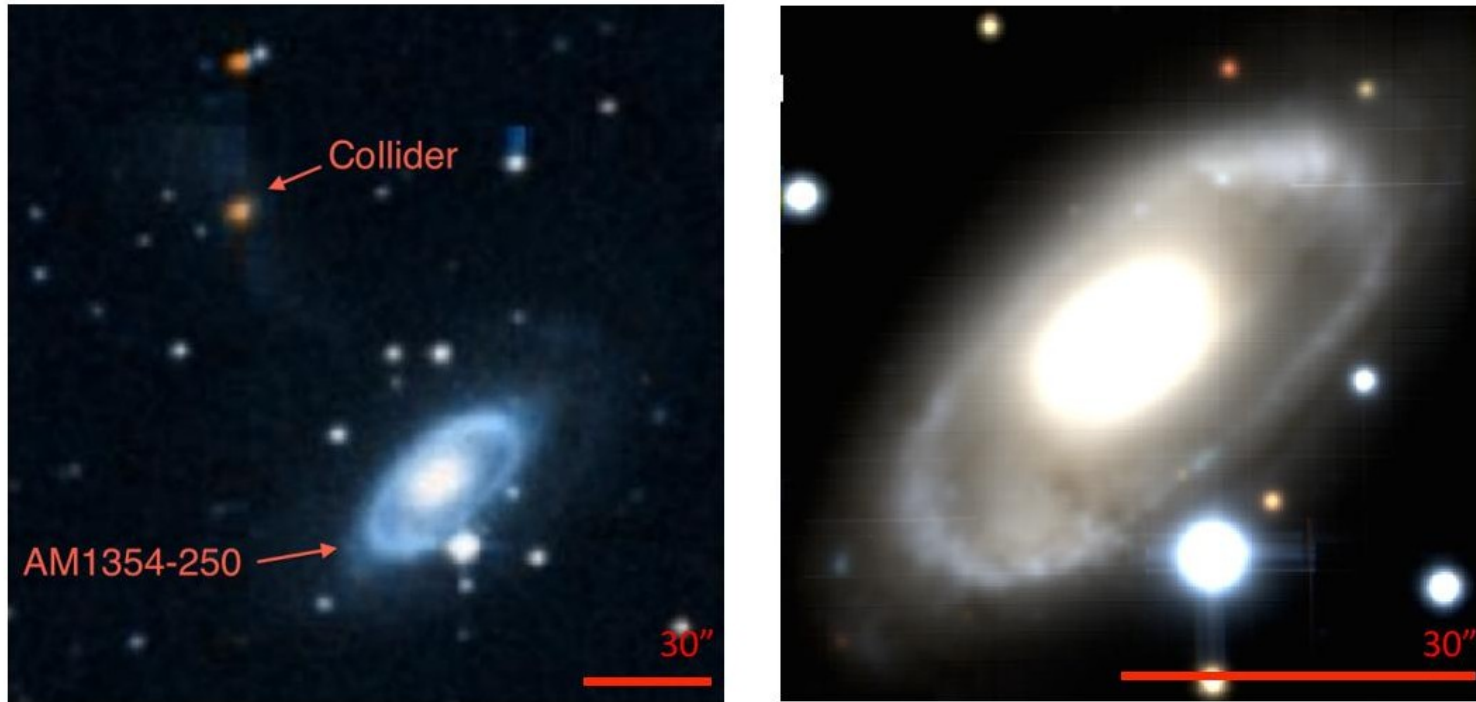
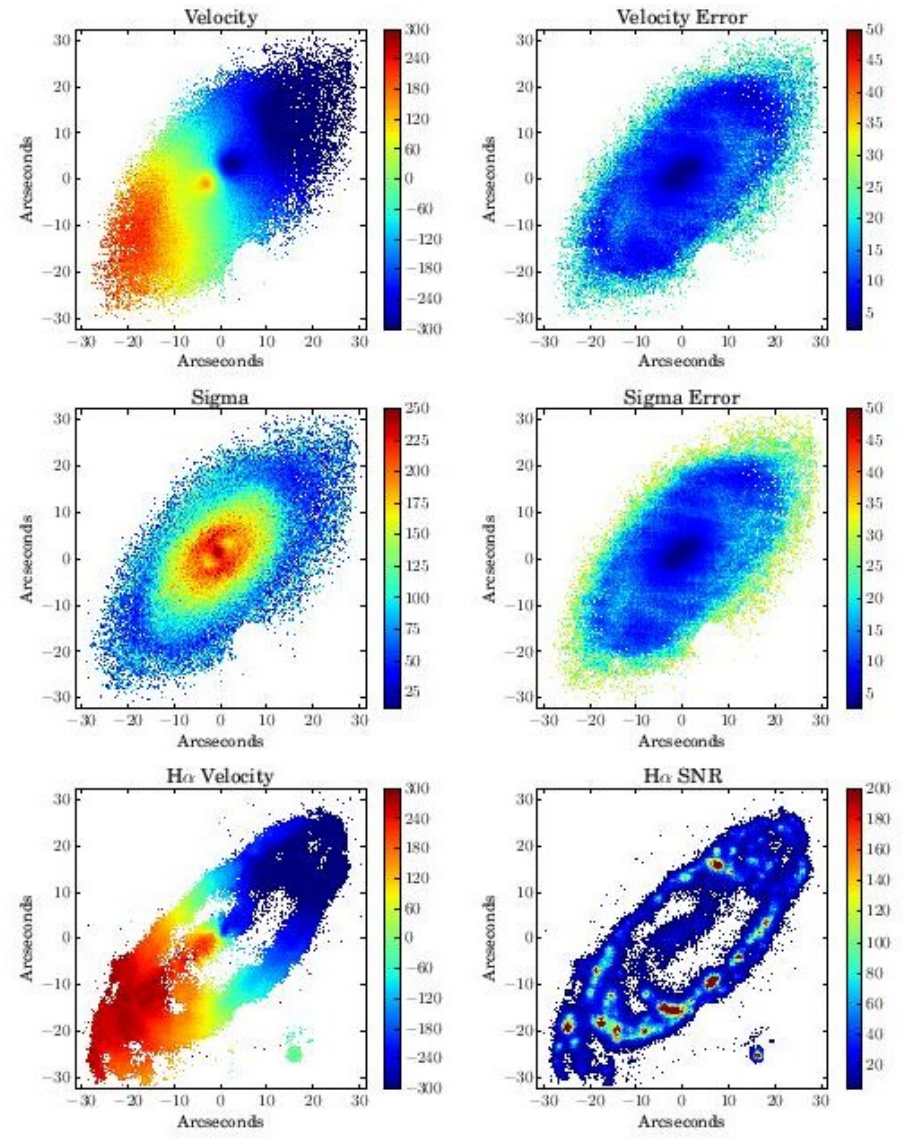


FIG. 1.— Left panel: HiPS color Digitized Sky Survey image<sup>a</sup>, showing AM1354-250 and its colliding galaxy. The ring of triggered star formation is clearly visible along with the diffuse outer disk and wispy tidal debris leading to the red core of the colliding galaxy. North is up and East is to the left. Right panel: False color RGB image generated from the reduced MUSE data cube by applying masks equivalent to SDSS<sup>b</sup>  $g$ ,  $r$  and  $i$  bands ( $R=i$ ,  $G=r$ ,  $B=g$ ). The color image has then been assembled using DS9<sup>c</sup>. The 0.2 by 0.2 arcsecond spaxels provide the highest resolution image of this galaxy to date. Easily visible are the dust lanes and remnant spiral structure of the galaxy. The disk appears to be warped. North is up and East is to the left.

# Результаты с MUSE: поля скоростей



# Модель с расширением:

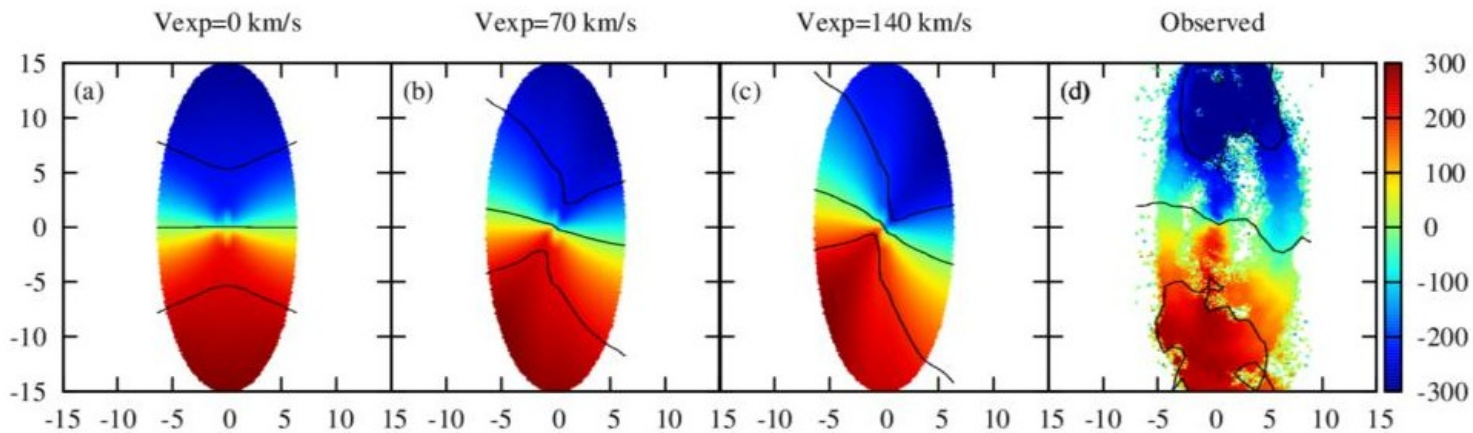


FIG. 10.— Panels (a), (b) and (c) illustrate the line-of-sight velocity field of a toy model disk with a circular velocity of  $320 \text{ km.s}^{-1}$ . In panel (a) the disk is purely rotating. In panel (b) and (c), a component of radial expansion is added to the disk dynamics. Contours are shown at  $-200 \text{ km.s}^{-1}$ ,  $0 \text{ km.s}^{-1}$ , and  $200 \text{ km.s}^{-1}$ . The velocity field twists clockwise with increasing expansion velocity. In panel (d), the  $\text{H}\alpha$  velocity map of AM1354-250 is shown, rotated anticlockwise by  $48^\circ$  to match the position angle of the toy model. The observed twist in the velocity field is approximated by an expansion velocity of  $\sim 70 \text{ km.s}^{-1}$ . This suggests that AM1354-250 is dominated by rotation, with a weak additional component of expansion.